Synthesis and characterization of silver nanoparticles by natural organic compounds extracted from Eucalyptus leaves and their role in the catalytic degradation of methylene blue d…

Article *in* Songklanakarin Journal of Science and Technology · March 2021

CITATIONS
0

READS
96

3 authors:

Muwafaq Rabeea
University of Anbar
21 PUBLICATIONS **65** CITATIONS
SEE PROFILE

Mustafa Nadhim Owaid
University of Anbar
81 PUBLICATIONS **560** CITATIONS
SEE PROFILE

Rasim Farraj Muslim
University OfAnbar
32 PUBLICATIONS **84** CITATIONS
SEE PROFILE

Songklanakarin J. Sci. Technol.
43 (1), 14-23, Jan. - Feb. 2021

http://www.sjst.psu.ac.th

Original Article

Synthesis and characterization of silver nanoparticles by natural organic compounds extracted from *Eucalyptus* leaves and their role in the catalytic degradation of methylene blue dye

Muwafaq Ayesh Rabeea[1], Mustafa Nadhim Owaid[2, 3*], and Rasim Farraj Muslim[3]

[1] *Department of Ecology, College of Applied Sciences-Hit, University of Anbar, Hit, Anbar, 31007 Iraq*

[2] *Department of Heet Education, General Directorate of Education in Anbar, Ministry of Education, Hit, Anbar, 31007 Iraq*

[3] *Department of Environmental Sciences, College of Applied Sciences-Hit, University of Anbar, Hit, Anbar, 31007 Iraq*

Received: 28 May 2019; Revised: 18 October 2019; Accepted: 22 October 2019

Abstract

The aim of this work is synthesis of AgNPs from cold and hot extracts of *Eucalyptus* leaves. After that, microwave irradiation has used to improve properties of these nanoparticles which applied to degrade methylene blue (MB) dye. The change in color of the mixture was from yellow to ruby-brown and to dark brown for the synthesized AgNPs from the cold extract (C-AgNPs) and the hot extract (H-AgNPs) of *Eucalyptus* leaves respectively. The biosynthesized H-AgNPs showed the highest absorbance at the beak of 440 nm compared as 430 nm for C-AgNPs. HM-AgNPs exhibited the smallest average of diameter reached 57.94 nm and the best degradation reached 71.34% compared with H-AgNPs (39.27%) after 24 h. The improved HM-AgNP using microwave irradiation was efficient in facilitating the degradation processes of the Azo-dye. This paper will lead to candidate suitable, cheap, eco-friendly and greener AgNPs for rapid degradation of damaging textile dyes.

Keywords: AFM, green synthesis, industrial applications, natural extracts, textile dye

1. Introduction

Nanotechnology is a used technique to synthesize different nanoparticles. Nanoparticles are defined as materials have different shapes and a specific size range from 1 to 100 nanometers (Vo-Dinh, 2005). Biosynthesis of metallic nanoparticles was exploited by reducing and stabilizing agents such as various enzymes and biomaterials, with physical and chemical methods to prepare the cheap, eco-friendly and non-toxic nanoparticles which so-called "Green Chemistry" (Sardar & Mazumder, 2019). In the last years, many researchers have used the biomaterials such as bacteria, fungi (Chan & Don, 2013), yeasts (Badhusha & Mohideen, 2016), mushrooms (Owaid, Al-Saeedi, & Abed, 2017; Owaid & Ibraheem, 2017; Owiad, 2019), and plants (Al-Bahrani, Muayad, Majeed, & Owaid, 2018; Owaid, Zaidan, & Muslim, 2019) to biosynthesize green nanoparticles. Recently, eco-friendly synthesis of AgNPs from plants was investigated and applied in the nanomedicine field (Muslim & Owaid, 2019; Rafique, Sadaf, Rafique, & Tahir, 2017). *Albizia procera* leaf extract was used to biosynthesize AgNPs which entered in important applications like degradation of dyes, and anti-bacterial activity (Rafique *et al.*, 2019). Also, the watery extract of *Allium giganteum* lowering shoots was used to biosynthesize green AgNPs which had photocatalytic effects, bactericidal activity, and cytotoxicity (Yazdi *et al.*, 2019).

*Corresponding author
Email address: mustafanowaid@gmail.com;
mustafanowaid@uoanbar.edu.iq

From another hand, *Eucalyptus* plant, a genus belongs for the family Myrtaceae, has active chemical compounds are including tannin, flavonoids, light oils (Cineole, Pinene, and phenolic acids), aldehydes and ketones (Hussein, 1985; Tovey & McDonald, 1997). The composition of *Eucalyptus corymbia* leaf extract contains a variety of bio-molecules responsible for the reduction of metal ions and stabilization of nanoparticles; among these bio-molecules are polyphenols and water-soluble heterocyclic compounds (Shan kar *et al*., 2004). Recently, Mo *et al.* (2015) has prepared spherical silver nanoparticles (AgNPs) with sizes from 4 to 60 nm by using leaf extract of *Eucalyptus*. Also, *Eucalyptus* leaf extract was used as a reducing and a capping agent to produce the AgNPs at the room temperature at sizes ranged from 30 to 36 nm (Balamurugan & Saravanan, 2017). El-Rahman and Tahany (2013) have used *Eucalyptus globulus* leaf extract to biosynthesize AgNPs. The synthesized AgNPs are predominantly spherical with sizes ranged from 9 to 32 nm. However, Sila *et al.* (2014) have used certain conditions at 90℃ and pH 5.7 to produce spherical AgNPs with sizes ranged from 18-20 nm without remarkable agglomeration.

Eucalyptus extract-assisted synthesis of spherical zinc oxide nanoparticles was carried out under ambient condition for the formation of spherical ZnO-NPs with a mean particle size of 11.6 nm. *Eucalyptus globulus* extract-mediated synthesis of spherical and crystalline ZnO-NPs with hexagonal structure also was achieved (Balaji & Kumar, 2017). Further, the biosynthesized AgNPs from methanol extracts of *Eucalyptus leucoxylon* were almost spherical in shape with an average diameter of ~50 nm within the reaction time of 120 min at the room temperature; these AgNPs were applied *in vitro* as antioxidant agents (AgNPs) (Rahimi-Nasrabadi, Pourmortazavi, Shandiz, Ahmadi, & Batooli, 2014).

Thus, this study tested biosynthesis and characteristics of silver nanoparticles from the cold and the hot extracts of *Eucalyptus* leaf and improving their proprties by using the microwave irradiation. Finally, all the synthesized AgNPs were invistigated for catalytic degradation of methylene blue (MB) dye.

2. Materials and Methods

2.1 Biomaterials

Eucalyptus sp. leaf samples were collected from the public garden in Hit, western Iraq. These leaves were cleaned, chopped to small pieces and extracted for use as a greener reducer of silver ions.

2.2 Extraction of *Eucalyptus* leaves

In this work, 10 g of chopped *Eucalyptus* leaves have extracted in 100 ml distilled water (DW). The first method involved crushing the leaves by the Blender at the room temperature 25 ℃ and stored in the freeze at -20 ℃ for two days then dissolved and filtered using gauze. The aqueous cold extract was centrifuged at 4,000 rpm for 15 min. This extract was used as a cold extract.

Another 10 g of chopped *Eucalyptus* leaves have extracted in 100 ml DW and heated at 80 ºC in a conical flask and then boiled for 1 h and left for the cooling. The aqueous hot extract was filtered using gauze, centrifuged at 4,000 rpm for 15 min and finally stored at 4 ºC for the next use. This extract was used as a hot extract in this investigation.

2.3 Biosynthesis of silver nanoparticles

Biosynthesis of silver nanoparticles was achieved by adding 1 ml of the two leaves extract (cold and hot extracts) with 10 ml (1 mM) $AgNO_3$ solution (Silver nitrate, 99.9 % Purity was prepared using Double Deionized water and purchased from Sigma Aldrich) separately, with stirring at 40 ℃ and 100 rpm for 30 min until the color of the solution changed. The prepared AgNPs were treated by employing microwave radiation at power 400 Watt for 5 min.

2.4 Characterization of the biosynthesized Ag nanoparticles

The prepared silver NPs from the hot and cold extracts of *Eucalyptus* leaves were characterized using the change of color in mixtures, UV-Vis spectroscopy, AFM, SPM, ZetaSizer, and FTIR, analyses.

2.5 Degradation of methylene blue dye

The two kinds of AgNPs were carried out for the degradation of methylene blue dye. One ml AgNPs colloid was mixed with 20 ml methylene blue (MB) dye solution (concentration of 10 ppm) with continuous shaking for 2, 4, 6 and 24 h at the temperature from 25-30 ℃ under dark condition. The residual solution absorbance is measured using UV-visible at ƛ max 664 nm. The degradation in MB was estimated by the following equation (Jyoti & Singh, 2016):

Degradation of MB % = $\frac{C_0 - C}{C} * 100$, where C_0 is the initial concentration of MB, C is the concentration of MB after degradation by Ag-NPs.

3. Results and Discussion

3.1 UV-Visible spectra of the extracts and their Ag nanoparticles

The first remarkable sign to the biosynthesis of silver nanoparticles is the change in color of the solution from yellow to ruby-brown and to dark brown color for the cold extract and the hot extract of *Eucalyptus* leaves respectively as shown in Figure 1. The change of color was seen after 30 minutes of the start of the reaction at the temperature of 40 ℃. The biosynthesized AgNPs from the hot extract shows the highest absorbance reaches 2.631 at the beak of 440 nm compared as the absorbance of 1.263 at the peak of 430 nm. The color of reaction becomes darker with the time because of excitation of Surface Plasmon Resonance (SPR) in AgNPs (Shankar, Ahmad, & Sastry, 2003) and that was affirmed by the UV–visible spectrum as in Figure 1. This result agrees with the result of the synthesis of AgNPs using the natural extract of oyster mushroom with 1 mM silver nitrate solution compared with the natural extract alone (Al-Bahrani, Raman, Lakshmanan, Hassan, & Sabaratnam, 2017; Owaid *et al.*, 2015).

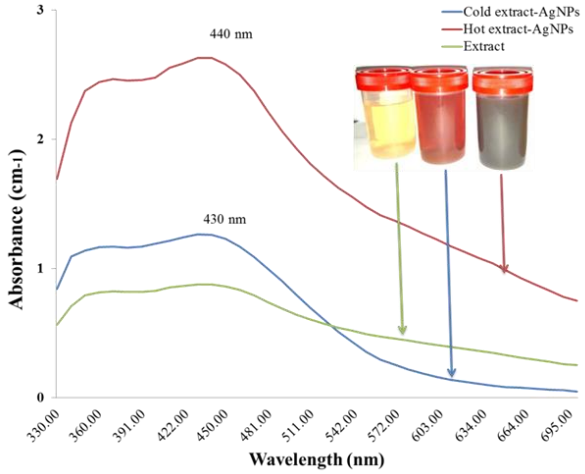

Figure 1. UV-Visible spectrum of the biosynthesized AgNPs and the extract of *Eucalyptus* leaves.

3.2 AFM of the AgNPs pre and post using the microwave irradiation

Atomic Force Microscope (AFM) images (Figure 2) shows the lateral (2D) and three-dimensional (3D) images to screen surface roughness of the biosynthesized silver nano-particles at size images 2012.46 nm×2030.59 nm for Cold Extract-AgNPs pre using Microwave (C-AgNPs), 2032.19 nm×2032.19 nm for Cold Extract-AgNPs post using Micro-wave (CM-AgNPs) (Figure 2A), 2046.98 nm×2046.98 nm for Hot Extract-AgNPs pre using Microwave (H-AgNPs) and 2019.62 nm×2074.20 nm for Hot Extract-AgNPs post using Microwave (HM-AgNPs) (Figure 2B). Surface roughness analysis shows some parameters such as amplitude, functional and hybrid parameters. Amplitude parameters have measured like roughness average reaches 1.37 nm, 0.39 nm, 1.06 nm, and 0.28 nm, and ten point height reaches 7.03 nm, 1.39 nm, 6.06 nm and 1.64 nm for Cold Extract-AgNPs pre (C-AgNPs) and post (CM-AgNPs) using Microwave, Hot Extract-AgNPs pre (H-AgNPs) and post (HM-AgNPs) using Microwave respectively. Functional parameters have measured such as reduced summit height reaches 1.94 nm, 0.32 nm, 0.54 nm, and 0.20 nm, core roughness depth reaches 3.94 nm, 1.36 nm, 3.54 nm, and 1.01 nm and reduced valley depth of 0.58 nm, 0.38 nm,1.80 nm and 0.27 nm for C-AgNPs and CM-AgNPs, H-AgNPs and HM-AgNPs respectively. Hybrid parameters have measured like surface area ratio which reaches 0.51, 0.11, 0.56, and 0.06 and root mean square slope reaches 0.10 nm^{-1}, 0.04 nm^{-1}, 0.10 nm^{-1}, and 0.3 nm^{-1} for C-AgNPs and CM-AgNPs, H-AgNPs and HM-AgNPs, respectively. This is an indicator for the formation of Ag nano-particles in small sizes in ≤90% of its NPs with diameters reach 110 nm, 75 nm, 85 nm and 70 nm for C-AgNPs and CM-AgNPs, H-AgNPs and HM-AgNPs respectively. Hot Extract-AgNPs post using Microwave (HM-AgNPs) exhibited best results as in Figure 2B compared as pre using the microwave (H-AgNPs) and as CM-AgNPs and C-AgNPs as in Figure 2A respectively. Therefore, Figure 2B (2D) showed the finest nanoparticles post using microwave. Effect of microwave irradiation appears through controlling Ag nanoparticle size and rate of reaction (Bhardwaj *et al.*, 2017). The microwave irradiation

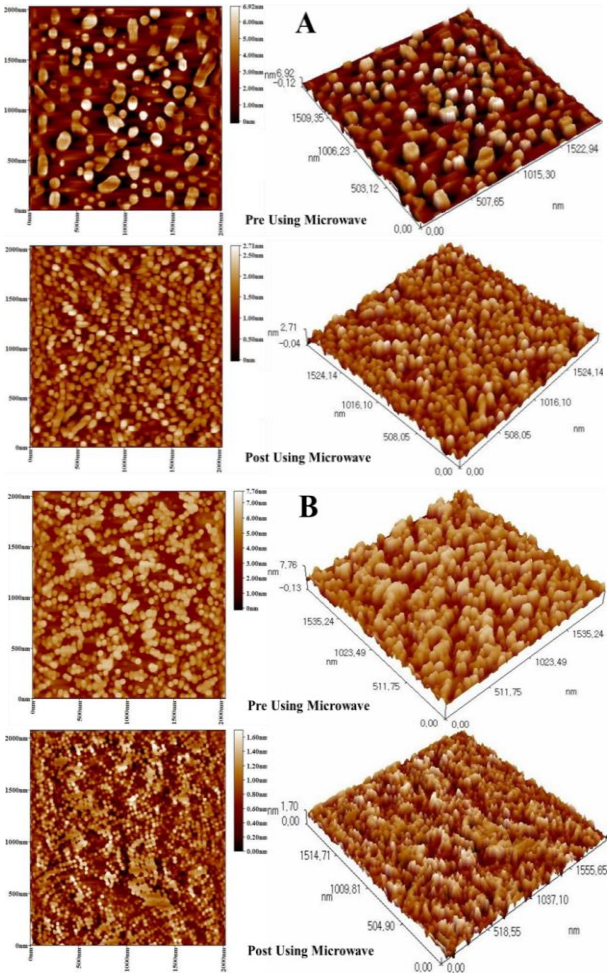

Figure 2. AFM [2D (lateral): on the left, and 3D (three dimensional): on the right] of the synthesized AgNPs pre and post using Microwave for 15 min at 25 °C, A: the cold extract-AgNPs, B: the hot extract-AgNPs.

leads to improve shapes and sizes of the synthesized AgNPs and gives small sizes during a short time (Saifuddin, Wong, & Yasumira, 2009).

3.3 ZetaSizer of the particle size distribution of AgNPs

Figure 3 exhibits histogram of the particle size distribution of the biosynthesized silver nanoparticles by using ZetaSizer. They are Cold Extract-AgNPs pre using Micro-wave irradiation (C-AgNPs), Cold Extract-AgNPs post using Microwave (CM-AgNPs), Hot Extract-AgNPs pre using Microwave (H-AgNPs) and Hot Extract-AgNPs post using Microwave (HM-AgNPs) as shown in Figures 3a-d, respec-tively. Averages of diameter are 91.49 nm, 65.55 nm, 72.36 nm, and 57.94 nm for C-AgNPs, CM-AgNPs, H-AgNPs, and HM-AgNPs, respectively. Volumes of C-AgNPs of 85 nm and 110 nm are ≤50%, and ≤90% respectively, while volumes of CM-AgNPs of 65nm and 75 nm are ≤50%, and ≤90%, respectively. Volumes of H-AgNPs of 65 nm and 85 nm are ≤50%, and ≤90% respectively, while volumes of HM-AgNPs

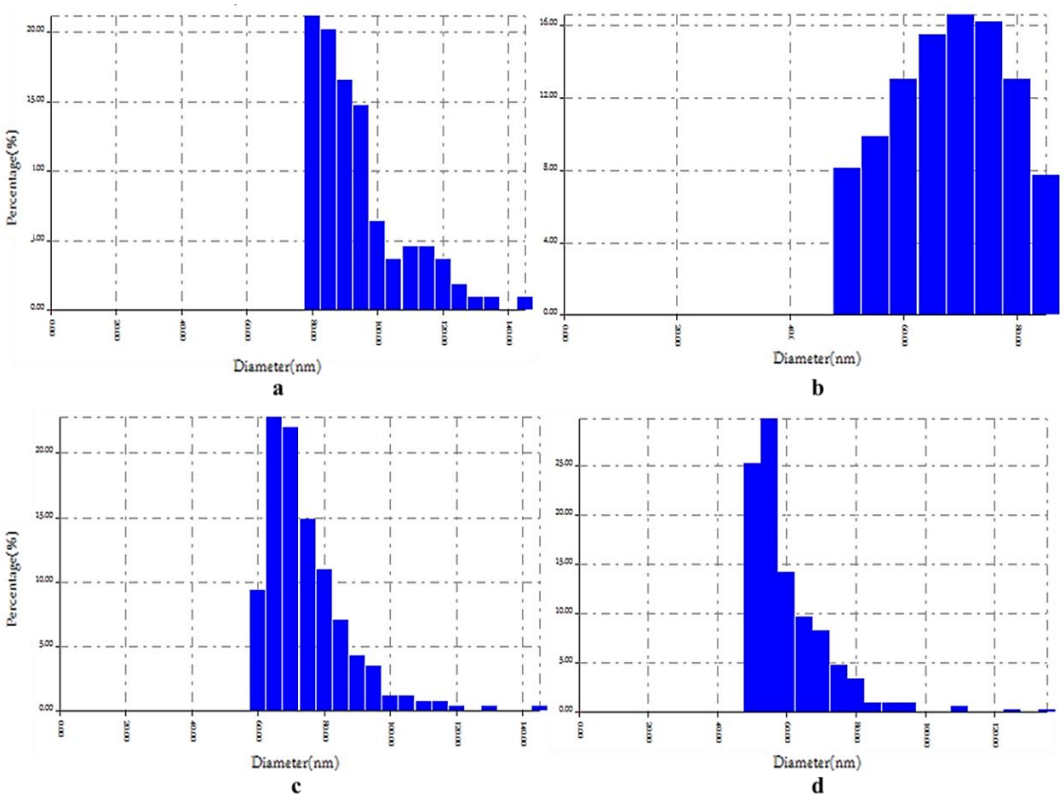

Figure 3. ZetaSizer of AgNPs distribution of cold extract-AgNPs colloid pre (a) and post using the microwave irradiation (b) and hot extract-AgNPs colloid pre (c) and post using the microwave for 15 min (d).

of 50 nm and 70 nm are ≤50%, and ≤90%, respectively. Lower nanoparticles diameter was 50 nm for HM-AgNPs and CM-AgNPs at volumes 25.26% and 8.10% respectively, while the higher diameter was 145 nm with volumes <1%. The higher amount is 29.76% for the HM-AgNPs with a diameter of 55 nm. Microwave-mediated biosynthesis method is used to control AgNPs sizes and volumes (Bhardwaj *et al.*, 2017). The results of this work agree with many recent studies which used combinatorial synthesis process for biosynthesis of AgNPs using microwave irradiation (Saifuddin *et al.*, 2009) and produced AgNPs with diameters from 40-70 from leaves of *Citrus sinensis* and *Origanum majorana* (Singh, Rawat, & Isha, 2016), 25-40 nm from *Fraxinus excelsior* leaves (Par veen, Ahmad, Malla, & Azaza, 2016) and from 20-50 nm from pods of *Parkia speciosa* Hassk (Fatimah, 2016). The use of microwave irradiation provides uniform heating around AgNPs without aggregation. The microwave irradiation heats up materials and converts the radiation energy into thermal energy. Not only the heating is faster through microwave irradiation, but also the distribution of the solution temperature is more uniform that lead to the fast reaction average and homogeneous silver nanoparticles with smaller sizes (Sai fuddin *et al*., 2009).

3.4 Granularity Cumulation distributions of the colloid AgNPs

Granularity cumulation distribution of AgNPs has also different accumulation according to their sizes as shown in Figure 4. The Ag nanoparticles of 50 nm have the lowest

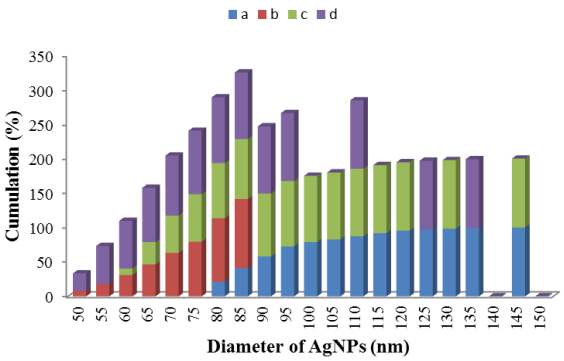

Figure 4. Granularity cumulation distributions of the colloid AgNPs.

accumulation of 8.10%, followed by 9.41% with diameters 60 nm for CM-AgNPs and H-AgNPs respectively. The higher accumulation percentage was 100% for C-AgNPs and H-AgNPs which have a size of 145 nm. Accumulation of AgNPs decreases according to smallness diameter of nanoparticles and increases according to the largeness diameter of nanoparticles (Owaid, Naeem, Muslim, & Oleiwi, 2020). The microwave irradiation leads to change compatibility and integrity of the shape and size of the biosynthesized AgNPs and gives a rapid green synthesis of AgNPs within 5 min (Saifuddin *et al*., 2009). Microwave-mediated biosynthesis approach is used to control nanoparticle size and rate of reaction (Bhardwaj *et al*., 2017), that is agreeing with the result of (Saifuddin *et al*., 2009) who referred to that the extract of

fungal culture and microwave irradiation were used together as a combinatorial synthesis process for the green synthesis of monodisperse AgNPs with low accumulation.

3.5 FT-IR spectrum illustration

In this study, six samples were selected from the extracts of *Eucalyptus* plants (Cold *Eucalyptus* Extract, Hot *Eucalyptus* Extract, and Cold Extract-AgNPs without using Microwave irradiation, Hot Extract-AgNPs without using Microwave, Cold Extract-AgNPs using Microwave and Hot Extract-AgNPs using Microwave). From Figures 5A and B, in the interpretation of infrared models of cold and hot extracts, the band 3,332 cm^{-1} in the cold extract, as shown in Figure 5A, belongs to the hydroxyl group (OH) which found in phenolic compounds such as Eucalyptin and polyphenols such as the Hyperin and Tannin (Figure 6) and the Trans-Pinocarveol compound. There is no such band in the hot extract, so it is likely that the heat evaporates these compounds from the hot extract by the heating (Abid, Tawfeeq, & Muslim, 2017; Muslim, Tawfeeq, Owaid, & Abid, 2018; Silverstein, Web ster, & Kiemle, 2005). It is noted that the band at site 1733 cm^{-1} for the cold extract indicates the presence of the carbonyl group (C=O) related to the Eucalyptin compound, the Hyperin compound, the Tannin compound, and flavonoids compounds. The band at site 1,741cm^{-1} for the hot extract indicates the presence of flavonoids.

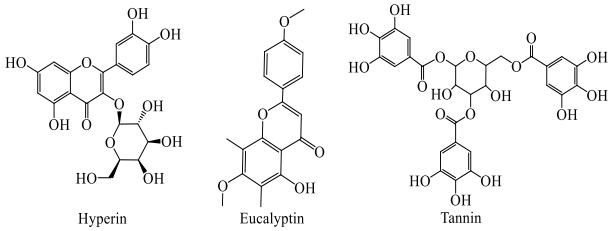

Figure 6. Structures of phenolic compounds.

The band at 1,614 cm^{-1} of the cold extract belong to the C=C group in the alkene compounds shown in the composition of Terpenine, Limonine, Pinene, and Trans-Pinocarveol. The band 1,613 cm^{-1} for the hot extract also belongs to the mentioned compounds except for Trans-Pinocarveol. The band 1,509 cm^{-1} of the cold extract belongs to the group C=C found in aromatic compounds such as Tannin, Eucalyptin, and Hyperin, also, flavonoids and Para-Cymene. The band at 1,460 cm^{-1} is also belonged to the compounds listed above, except Tannin, Eucalyptin, and Hyperin. The band at 1,063 cm^{-1} of the cold extract belongs to C-C while the two bands at 2,885 cm^{-1} and 2,920 cm^{-1} of the hot extract belong to the homogeneous and heterogeneous extension vibrations for the methylene group ($-CH_2$) or the methyl group ($-CH_3$) in the composition Eucalyptin (Figure 6), Trans-Pinocarveol, Terpinene, Pinene and Limonene, 1, 3,

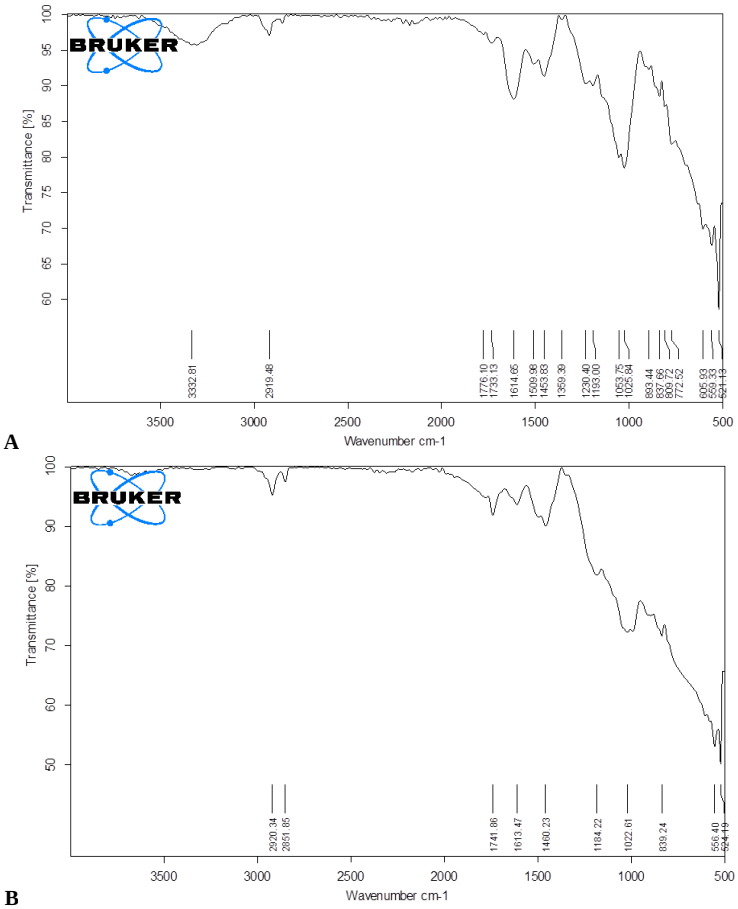

Figure 5. FT-IR spectra of the cold extract (A) and the hot extract (B) of *Eucalyptus* leaves.

3- trimethyl- 2- oxabicyclo [2.2.2] octane, (1*s*,4*s*)-1-isopropyl- 4- methyl- 7- oxabicyclo [2.2.1] heptane, Para-Cymene and 1,8-Cineole. But the band at 1,022 cm^{-1} for the hot also belongs to the mentioned compounds except the compounds containing the hydroxyl group (OH). The band at 1,776 cm^{-1} for the cold extract supports the presence of the Lactone group (O-C=O) finds in one of the flavonoids.

Silver nanoparticles of the cold and hot extracts without microwave appear in Figures 7A and B respectively. The previous silver nanoparticles contain almost identical bands in terms of the site of the bands mentioned in the FT-IR of the two extracts in Figures 5A and B. In addition, the hot extract-silver nanoparticles contain a wide band at 3,207 cm^{-1}; this confirms the presence of hydroxyl groups in this AgNPs compared with its hot extract (Figure 5B). This means that the hot extract-AgNPs contain phenolic compounds such as Eucalyptin and polyphenols such as the Hyperin, Tannin and the Trans-Pinocarveol compound. In addition to the fact that the bands in both Figures 7A and B are clearer and more stretchable; it is believed that due to the good distribution of silver nanoparticles, that led to the active groups are free to move, be it bending or vibration.

The silver nanoparticles of the cold and hot extracts using microwave appear in Figures 8A and B, respectively. It is noted that the hot extract-AgNPs using the microwave has missed the hydroxyl group (OH). It is believed that the microwave heat is the cause; therefore, this sample does not contain mono hydroxyl and poly hydroxyl phenols. From another hand, the hot extract-AgNPs using microwave has retained this group (OH) at the site 3,202 cm^{-1} unlike the cold extract-AgNPs using the microwave and therefore this nanoparticle can be considered the best among the other nanoparticles as has not lost any of the active compounds of the *Eucalyptus* extract (Owaid, Muslim, & Hamad, 2018).

Here, the clarity of the bands shown in Figures 8A and B have clearly been shown. This demonstrates that the silver nanostructure causes better clarity of the bands due to the small granular size and thus increasing the surface area exposed to the infrared radiation. All these are leading to a better arrangement of the functional groups within the empty

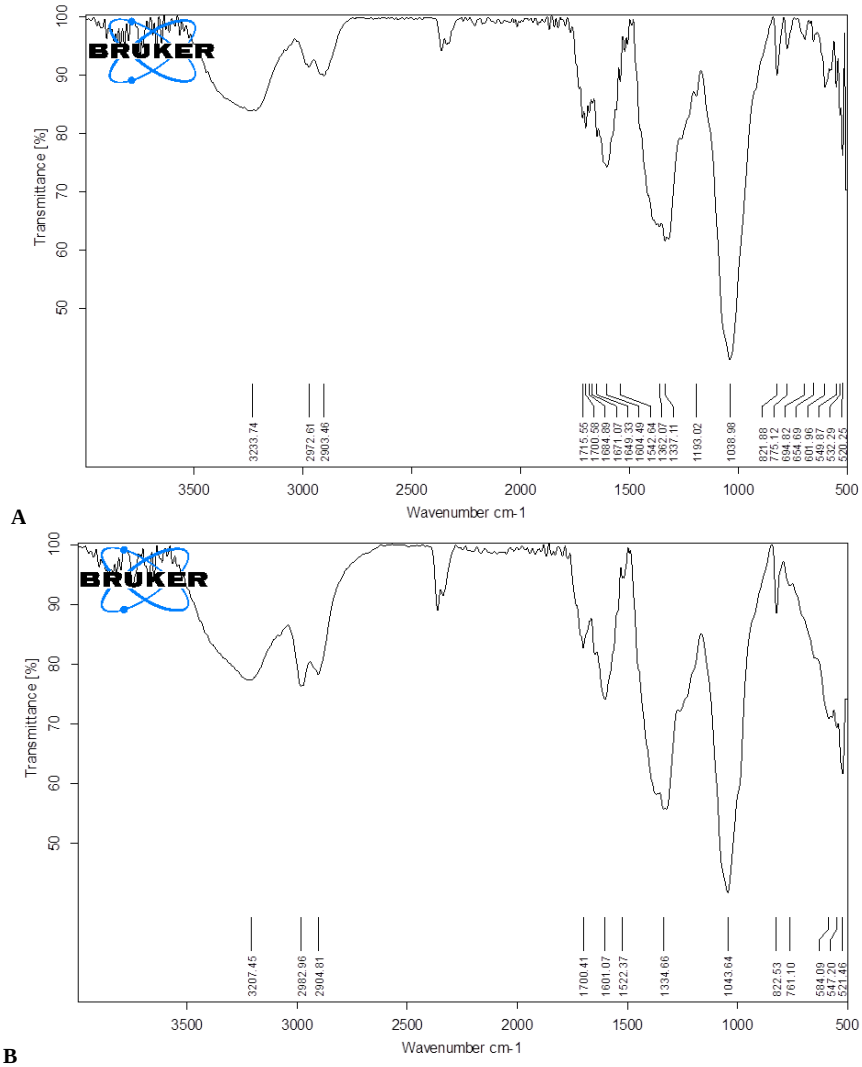

Figure 7. FTIR spectra of the cold extract-AgNPs (C-AgNPs) (A) and the hot extract-AgNPs (H-AgNPs) (B) without microwave.

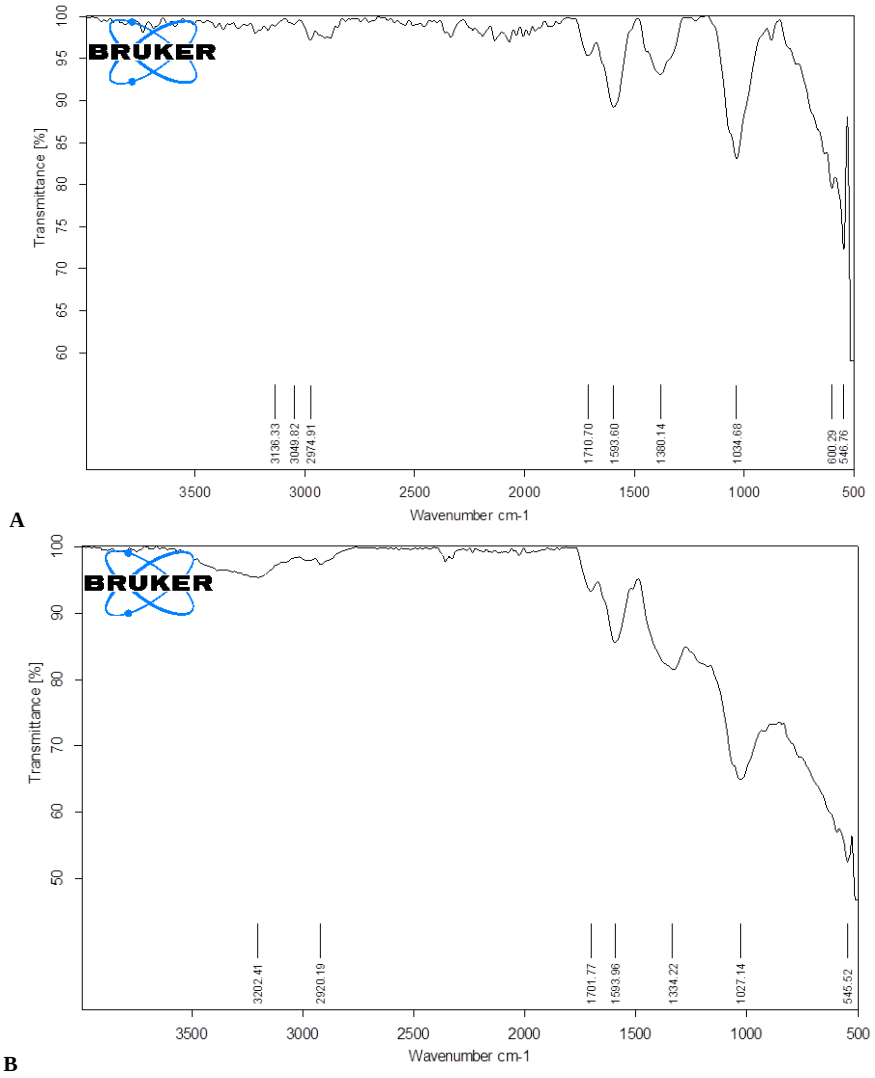

Figure 8. FTIR spectra of the cold extract-AgNPs (CM-AgNPs) (A) and the hot extract-AgNPs (HM-AgNPs) (B) using microwave.

orbitals of the silver atoms. The reason for the clarity of the bands of silver nanoparticles may be due to the presence of silver atoms with a good surface area that allows all atoms with high electrolytes containing non-participating electronic pairs, such as the oxygen atom to give these pairs to empty orbitals in silver atoms. The link is as follows (Ag-O-R) where R is mono hydroxyl phenols, poly hydroxyl phenols or flavonoids or other compounds containing the oxygen atom, so the consistency between the main compounds in the composition of *Eucalyptus* extract with empty orbitals in the composition of silver atoms may gain freedom in vibration of functional groups and thus stretch and clarity to appear good. The functional groups are responsible for reducing Ag ions and forming AgNPs by using microwave can be proteins and phenols as in the extract of leaves of *Citrus sinensis* and *Origanum majorana* (Singh *et al*., 2016), or glycosides, amino acid residues, peptides, phenolic compounds, flavonoids, alkaloids and terpenoids of *Fraxinus excelsior* leaves (Parveen, Ahmad, Malla, & Azaza, 2016).

3.6 Degradation of methylene blue using AgNPs

The catalytic activity of synthesized *Eucalyptus*-mediated AgNPs was analyzed for degradation of methylene blue (MB) dye under dark condition. Figure 9 shows the degradation percentage of methylene blue using hot *Eucalyptus* extract-AgNPs pre and post using the microwave at different times. The catalytic degradation of MB was determined by the decreasing intensity of the absorption band. The colors of the mixed dye with AgNPs were gradually changed with time from deep blue to light blue compared with the MB alone which stay deep blue (control). In general, hot extract-AgNPs using microwave exhibited higher degradation of the Azo dye compared with hot extract-AgNPs without using microwave irradiation because of the smaller diameter of AgNPs exposed to microwave irradiation. Increasing the time of incubation led to increasing the degradation percentage of methylene blue. HM-AgNPs exhibited best degradation reached 71.34% compared with H-AgNPs (39.27%) after 24 h

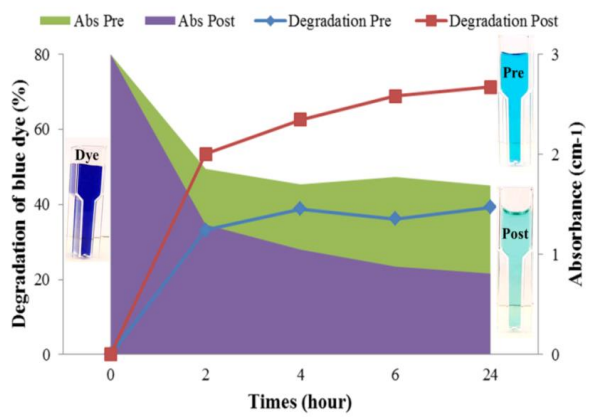

Figure 9. Degradation of methylene blue dye using HM-AgNPs and CM-AgNPs.

of incubation time, while HM-AgNPs exhibited degradation percentage 53.50% compared as the lowest degradation reached 33.18% by H-AgNPs pre using microwave irradiation after 2 h. The improved HM-AgNP using microwave irradiation was efficient in facilitating the degradation processes of the Azo-dye. The mechanism of degradation of MB is relating to the organic matters on the surface of AgNPs. The electron transfer takes place from the reducing agent (natural products of *Eucalyptus*) to dye molecule via AgNPs (Saravanan, Rajesh, & Kaviarasan, 2017), resulting in the destruction of the industrial textile dye chromophore structure. Degradation of the blue dye was not found to proceed in the absence of either HM-AgNPs or H-AgNPs catalysts. Azo dyes bearing the functional group R–N=N–R is widely used in textile and reduced to colorless amines (–NH–NH–) in the presence of HM-AgNPs as a catalyst (Rasheed *et al.*, 2018). Figure 9 exhibits the catalytic degradation of the blue dye with time. The enhanced degradation by HM-AgNP as a nanocatalyst can be ascribed to the high surface area can absorb the dye, and the AgNPs catalysts are expected to activate the Azo nitrogen bond and also to bind with the sulfur and oxygen atoms of the dye resulting in weakening of Azo double bond via conjugation, which helps in bringing the blue dye molecules near the catalytic sites (Saravanan *et al.*, 2017). Also, Figure 9 confirms that the HM-AgNP is observed to be an excellent catalyst on reduction of the hazardous dyes like MB, which is confirmed by decreasing absorbance (Jyoti & Singh, 2016) and changing the dark blue color to the bright blue as an indicator to success role of AgNPs to degrade and reduce the Azo-dyes (Santhosh, Sandeep, & Swamy, 2019). The reduction of methylene blue by AgNPs agrees with the results of (Hamedani & Hekmati, 2019; Joshi, Geetha, Al-Mamari, & Al-Azkawi, 2018). Finally, the degradation of MB increased with decrease in the size of AgNPs due to the increase in the number of reaction sites (Muthukrishnan *et al.*, 2015). Also, the biosynthesized AgNPs are playing as catalysts in reducing MB by natural organic matters of *Eucalyptus* which found on the surface of Ag nanoparticles.

4. Conclusions

The aim of this work is the synthesis of AgNPs from cold and hot extracts of *Eucalyptus* leaves. The microwave irradiation has used to improve properties of these nanoparticles which applied to degrade methylene blue dye. FTIR showed some functional groups like -OH which missed after using microwave irradiation; also Flavonoids, Tannin, Eucalyptin, and Hyperin may be reduced Ag^{+} to the silver atom. The biosynthesized H-AgNPs show the highest absorbance at the beak of 440 nm. HM-AgNPs exhibited the smallest average of diameter reached 57.94 nm. HM-AgNPs exhibited the best degradation reached 71.34% after 24 h. The degradation of MB increased with decrease in the size of AgNPs. Finally, the biosynthesized AgNPs are playing as catalysts in reducing MB by natural organic matters of *Eucalyptus*.

References

Abid, O. H., Tawfeeq, H. M., & Muslim, R. F. (2017). Synthesis and characterization of novel 1, 3-oxazepin-5(1H)-one derivatives via reaction of imine compounds with isobenzofuran-1(3H)-one. *Acta Pharmaceutica Sciencia*, *55*, 43–55.

Al-Bahrani, R. M., Muayad, S., Majeed, A., & Owaid, M. N. (2018). Phyto-fabrication, characteristics and anti-candidal effects of silver nanoparticles from leaves of *Ziziphus mauritiana* Lam. *Acta Pharmaceutica Sciencia*, *56*(3), 85–92.

Al-Bahrani, R., Raman, J., Lakshmanan, H., Hassan, A. A., & Sabaratnam, V. (2017). Green synthesis of silver nanoparticles using tree oyster mushroom *Pleurotus ostreatus* and its inhibitory activity against pathogenic bacteria. *Materials Letters*, *186*, 21–25.

Badhusha, M. S. M., & Mohideen, M. M. A. K. (2016). Biosynthesis of silver nanoparticles using *Saccharomyces cerevisiae* with different pH and study of antimicrobial activity against bacterial pathogens. *Chemical Science Transactions*, *5*(4), 906–911.

Balaji, S., & Kumar, M. (2017). Facile green synthesis of zinc oxide nanoparticles by *Eucalyptus globulus* and their photocatalytic and antioxidant activity. *Advanced Powder Technology*, *28*(3), 785–797.

Balamurugan, M., & Saravanan, S. (2017). Green synthesis of silver nanoparticles by using *Eucalyptus globulus* leaf extract. *Journal of The Institution of Engineers (India): Series A*, *98*(4), 461–467.

Bhardwaj, A. K., Shukla, A., Mishra, R. K., Singh, S., Mishra, V., Uttam, K. N., Singh, M.P., . . . Gopal, R. (2017). Power and time-dependent microwave assisted fabrication of silver NPs decorated cotton (SNDC) fibres for bacterial decontamination. *Frontiers in Microbiology*, *8*, 330.

Chan, Y. S., & Don, M. M. (2013). Biosynthesis and structural characterization of Ag nanoparticles from white rot fungi. *Materials Science and Engineering C*, *33*(1), 282–288.

El-Rahman, A. F. A., & Mohammad, T. G. M. (2013). Green synthesis of silver nanoparticle using *Eucalyptus globulus* leaf extract and its antibacterial activity. *Journal of Applied Sciences Research*, *9*(10), 6437–6440.

Fatimah, I. (2016). Green synthesis of silver nanoparticles using extract of *Parkia speciosa* Hassk pods assisted by microwave irradiation. *Journal of Advanced Research*, *7*, 961–969.

Hamedani, Y. P., & Hekmati, M. (2019). Green biosynthesis of silver nanoparticles decorated on multi-walled carbon nanotubes using the extract of *Pistacia atlantica* leaves as a recyclable heterogeneous nanocatalyst for degradation of organic dyes in water. *Polyhedron*, *164*, 1–6.

Hussein, F. T. K. (1985). *Medicinal plants in Libya* (1st ed.). Hazmieh, Lebanon: Arab Encyclopedia House.

Joshi, S. J., Geetha, S. J., Al-Mamari, S., & Al-Azkawi, A. (2018). Green synthesis of silver nanoparticles using pomegranate peel extracts and its application in photocatalytic degradation of methylene blue. *Jundishapur Journal of Natural Pharmaceutical Products*, *13*(3), e67846.

Jyoti, K., & Singh, A. (2016). Green synthesis of nanostructured silver particles and their catalytic application in dye degradation. *Journal of Genetic Engineering and Biotechnology*, *14*(2), 311–317.

Mo, Y.-Y., Tang, Y.-K., Wang, S.-Y., Lin, J.-M., Zhang, H.-B., & Luo, D.-Y. (2015). Green synthesis of silver nanoparticles using *Eucalyptus* leaf extract. *Materials Letters*, *144*, 165–167.

Muslim, R. F., Tawfeeq, H. M., Owaid, M. N., & Abid, O. H. (2018). Synthesis, characterization and evaluation of antifungal activity of seven-membered heterocycles. *Acta Pharmaceutica Sciencia*, *56*(2), 39–57.

Muslim, R. F., & Owaid, M. N. (2019). Synthesis, characterization and evaluation of the anti-cancer activity of silver nanoparticles by natural organic compounds extracted from *Cyperus* sp. rhizomes. *Acta Pharmaceutica Sciencia*, *57*(2), 129–146.

Muthukrishnan S, B. S., Muthukumar M, S. M., & Rao MV, S. K. T. (2015). Catalytic degradation of organic dyes using synthesized silver nanoparticles: A green approach. *Journal of Bioremediation and Biodegradation*, *6*(5), 1000312.

Owaid, M. N., Al-Saeedi, S. S. S., & Abed, I. A. (2017). Biosynthesis of gold nanoparticles using yellow oyster mushroom *Pleurotus cornucopiae* var. *Citrinopileatus*. *Environmental Nanotechnology, Monitoring and Management*, *8*, 157–162.

Owaid, M. N., & Ibraheem, I. J. (2017). Mycosynthesis of nanoparticles using edible and medicinal mushrooms. *European Journal of Nanomedicine*, *9*(1), 5–23.

Owaid, M. N. (2019). Green synthesis of silver nanoparticles by *Pleurotus* (oyster mushroom) and their bioactivity: Review. *Environmental Nanotechnology, Monitoring and Management*, *12*, 100256.

Owaid, M. N., Naeem, G. A., Muslim, R. F., & Oleiwi, R. S. (2020). Synthesis, characterization and antitumor efficacy of silver nanoparticle from *Agaricus bisporus* pileus, Basidiomycota. *Walailak Journal of Science and Technology*, *17* (Online).

Owaid, M. N., Raman, J., Lakshmanan, H., Al-Saeedi, S. S. S., Sabaratnam, V., & Ali, I. A. (2015). Mycosynthesis of silver nanoparticles by *Pleurotus cornucopiae* var. *citrinopileatus* and its inhibitory effects against *Candida* sp. *Materials Letters*, *153*, 186–190.

Owaid, M. N., Muslim, R. F., & Hamad, H. A. (2018). Mycosynthesis of silver nanoparticles using *Terminia* sp. desert truffle, Pezizaceae, and their antibacterial activity. *Jordan Journal of Biological Sciences*, *11*(4), 401–405.

Owaid, M. N., Zaidan, T. A., & Muslim, R. F. (2019). Biosynthesis, characterization and cytotoxicity of zinc nanoparticles using *Panax ginseng* Roots, Araliaceae. *Acta Pharmaceutica Sciencia*, *57*(1), 19–32.

Parveen, M., Ahmad, F., Malla, A. M., & Azaza, S. (2016). Microwave-assisted green synthesis of silver nanoparticles from *Fraxinus excelsior* leaf extract and its antioxidant assay. *Applied Nanoscience*, *6*, 267–276.

Rafique, M., Sadaf, I., Rafique, M. S., & Tahir, M. B. (2017). A review on green synthesis of silver nanoparticles and their applications. *Artificial Cells, Nanomedicine, and Biotechnology*, *45*(7), 1272–1291.

Rafique, M., Sadaf, I., Tahir, M. B., Rafique, M. S., Nabi, G., Iqbal, T., & Sughra, K. (2019). Novel and facile synthesis of silver nanoparticles using *Albizia procera* leaf extract for dye degradation and antibacterial applications. *Materials Science and Engineering: C*, *99*, 1313–1324.

Rahimi-Nasrabadi, M., Pourmortazavi, S. M., Shandiz, S. A. S., Ahmadi, F., & Batooli, H. (2014). Green synthesis of silver nanoparticles using *Eucalyptus leucoxylon* leaves extract and evaluating the antioxidant activities of extract. *Natural Product Research Formerly Natural Product Letters*, *28*(22), 1964–1969.

Rasheed, T., Bilal, M., Li, C., Nabeel, F., Khalid, M., & Iqbal, H. M. N. (2018). Catalytic potential of biosynthesized silver nanoparticles using *Convolvulus arvensis* extract for the degradation of environmental pollutants. *Journal of Photochemistry and Photobiology, B: Biology*, *181*, 44–52.

Saifuddin, N., Wong, C. W., & Yasumira, A. A. N. U. R. (2009). Rapid biosynthesis of silver nanoparticles using culture supernatant of bacteria with microwave irradiation. *E-Journal of Chemistry*, *6*(1), 61–70.

Santhosh, A. S., Sandeep, S., & Swamy, N. K. (2019). Green synthesis of nano silver from *Euphorbia geniculata* leaf extract: Investigations on catalytic degradation of Methyl orange dye and optical sensing of Hg2+. *Surfaces and Interfaces*, *14*, 50–54.

Saravanan, C., Rajesh, R., & Kaviarasan, T. (2017). Synthesis of silver nanoparticles using bacterial exopolysaccharide and its application for degradation of azo-dyes. *Biotechnology Reports*, *15*, 33–40.

Sardar, M., & Mazumder, J. A. (2019). Biomolecules assisted synthesis of metal nanoparticles. In N. D. *et al.* (Ed.), *Environmental Nanotechnology, Environmental Chemistry for a Sustainable World 21* (pp. 1–23). Cham, Switzerland: Springer Nature Switzerland AG.

Shankar, S. S., Ahmad, A., & Sastry, M. (2003). Geranium leaf assisted biosynthesis of silver nanoparticles. *Biotechnology Progress*, *19*, 1627–1631.

Shankar, S. S., Rai, A., Ankamwar, B., Singh, A., Ahmad, A., & Sastry, M. (2004). Biological synthesis of triangular gold nanoprisms. *Nature Materials*, *3*(7),

482–488.

Sila, J. M., Kiio, I., Mwaura, F. B., Michira, I., Abongo, D., Iwuoha, E., & Kamau, G. N. (2014). Green synthesis of silver nanoparticles using *Eucalyptus corymbia* leaves extract and antimicrobial applications. *International Journal of BioChemiPhysics*, *22*, 21-30.

Silverstein, R., Webster, F., & Kiemle, D. (2005). *Spectrometric identification of organic compounds* (7th ed.). London, England: John Wiley and Sons.

Singh, D., Rawat, D., & Isha, B. (2016). Microwave-assisted synthesis of silver nano-particles from *Origanum majorana* and *Citrus sinensis* leaf and their antibacterial activity: A green chemistry approach. *Bioresources and Bioprocessing*, *3*(1), 14.

Tovey, E. R., & McDonald, L. G. (1997). Clinical aspects of allergic disease: A simple washing procedure with *Eucalyptus* oil for controlling house dust mites and their allergens in clothing and bedding. *Journal of Allergy and Clinical Immunology*, *100*, 464–467.

Vo-Dinh, T. (2005). *Protein nanotechnology, protocols, instrumentation, and applications*. Totowa, NJ: Humana Press.

Yazdi, M. E. T., Hamidi, A., Amiri, M. S., Kazemi O. R., Hosseini, H. A., Hashemzadeh, A., & Darroudi, M. (2019). Eco-friendly and plant-based synthesis of silver nanoparticles using *Allium giganteum* and investigation of its bactericidal, cytotoxicity, and photocatalytic effects. *Materials Technology*, *34*(8), 490–497.